

LRP 365/88

December 1988

Density measurement of a magnetized Plasma
column using a resonant cavity technique

P.J. Paris, M.L. Sawley, M.Q. Tran and K. Voser

DENSITY MEASUREMENT OF A MAGNETIZED PLASMA COLUMN USING A RESONANT CAVITY TECHNIQUE

P.J. Paris, M.L. Sawley,* M.Q. Tran and K. Voser +

Centre de Recherches en Physique des Plasmas
Association Euratom - Confédération Suisse
Ecole Polytechnique Fédérale de Lausanne
21, Av. des Bains, CH-1007 Lausanne, Switzerland

ABSTRACT

A study of the application of high order TM_{0m0} modes of a cylindrical cavity to the measurement of the density of a magnetized plasma column is presented. It is shown theoretically that judiciously chosen high order modes have the potential advantages of both a wide operational range of densities, and a wide range for which a simple perturbation theory is valid. Furthermore, an experiment is described which shows that the TM_{060} mode can be excited with a sufficiently high Q value to allow accurate determination of the resonant frequencies, and hence plasma density. Favourable comparison between densities in the range 10^{10} - 10^{12} cm⁻³ measured by means of the resonant cavity technique and microwave interferometry is presented.

Present address:

* I.M.H.E.F. - E.P.F.L., ME - Ecublens, CH-1015 Lausanne, Switzerland
+ Organisation Zoller SA, CH-1800 Vevey, Switzerland

I. Introduction

Many plasma physics experiments can be investigated using a cold, low density, magnetized plasma. Among the advantages of these devices are their low cost, the low power levels and relatively easy handling of the different apparatus required for operation, and the low level of sophistication necessary in the diagnostics. Such devices are of interest in the study of fundamental plasma physics and as an introduction to experimental plasma research. In this spirit, we describe here a method to measure the average plasma density which is non-perturbative and applicable for a wide range of densities.

For low density plasmas, Langmuir probes are generally used to measure the plasma density. Langmuir probe characteristics obtained in a magnetized plasma are, however, difficult to interpret and an accurate measurement of density is only obtained after the careful consideration of various correction effects [1,2]. For a magnetized plasma, it is therefore traditional to calibrate the density profiles deduced from Langmuir probe data with absolute line-integrated density measurements obtained from microwave interferometry. Due to the limitation in measuring small fringe shifts, the application of microwave interferometry is generally restricted to a range of sufficiently high densities. In addition, the need in some cases to introduce antennas into the discharge vessel, may prohibit the use of interferometry. Microwave interferometry also requires components, such as a high frequency generator, sensitive phase shifter and detectors, that may not be readily available in a small laboratory for the dedicated purpose of density measurement. It may therefore be beneficial, or necessary, to consider an alternative diagnostic technique to provide absolute density measurements.

A possible alternative is the resonant cavity technique, in which changes in the resonant frequencies of a cavity surrounding the plasma can be related to changes in the plasma density. Such a diagnostic is simple in concept, and has been first described over thirty years ago. This technique has the possible advantage of

requiring a generator of lower frequency than needed for interferometry. In addition, the cavity is easily introduced into the vacuum vessel, or made part of a metallic vacuum vessel.

A number of theoretical and experimental investigations of the application of a resonant cavity to the measurement of plasma density have been made [see, for example, Ref. 3 - 10]. For a magnetized plasma column, a TM_{0m0} mode is generally considered since the cavity wavefields (neglecting end effects) are not influenced by the external magnetic field. A low order mode, usually $m = 1$, has invariably been used for previously reported measurements. Modes of higher order than $m = 2$ have not appeared to receive any attention in the literature.

The resonant cavity technique can, in principle, be applied over a wide range of densities. In practice, however, measurements are limited to densities below the critical density n_c for which the plasma frequency equals the resonant frequency of the cavity. As noted by Chen et al. [9], for $n > n_c$ the cavity Q is generally not sufficiently high to provide an accurate determination of the resonant frequency. Since the resonant frequency increases with mode number m , the critical density is also greater for higher order modes.

For a given experimental plasma device, the choice of a low order mode is therefore not appropriate if the density is greater than the critical density for that mode. In addition, the constraint of the use of an available high frequency generator may necessitate, for example, the consideration of a mode of high order. In this paper, we present a detailed theoretical analysis of the application of high order modes to the measurement of plasma density. Consideration is made here of the influence of the finite cavity length, as well as the plasma non-uniformity. Results are also presented of an experiment in which the TM_{060} mode was used to measure the density of a steady-state magnetized plasma column.

2. Theory

We shall consider a cylindrical cavity of radius a and length d that surrounds a plasma column of radius R , as shown in Fig. 1. The present study, which is concerned only with the diagnostic application of the cavity, shall be confined to the excitation of the TM_{0m0} modes.

It can be shown [5,7] that the resonant frequency ω of the cavity surrounding a plasma having a uniform density with a corresponding plasma frequency ω_p , is given by

$$\frac{k^2}{k_0^2} (\alpha - \beta) = \frac{2\gamma}{k_0 R} \quad (1)$$

where

$$\alpha = \frac{2 J_1(kR)}{kR J_0(kR)} \quad (2)$$

$$\gamma = \frac{J_1(k_0 R) N_0(k_0 a) - N_1(k_0 R) J_0(k_0 a)}{J_0(k_0 R) N_0(k_0 a) - N_0(k_0 R) J_0(k_0 a)} \quad (3)$$

$$\text{and } k_0^2 = \frac{\omega^2}{c^2}, \quad k^2 = \left(1 - \frac{\omega_p^2}{\omega^2} \right) k_0^2.$$

J_n and N_n are the Bessel functions of first and second kind.

In Eq. (1), the term β expresses the correction due to the fringing fields at the ends of the finite length cavity. Using the development of Thomassen [6], it can be shown that

$$\beta = \begin{cases} \frac{4R}{d} \sum_n \frac{1 - \exp\left[-\frac{d(p_n^2 - k^2 R^2)^{1/2}}{R}\right]}{(p_n^2 - k^2 R^2)^{3/2}} & \text{if } p_n^2 > k^2 R^2 \\ \frac{4R}{d} \sum_n \frac{\sin\left[-\frac{d(k^2 R^2 - p_n^2)^{1/2}}{R}\right]}{(k^2 R^2 - p_n^2)^{3/2}} & \text{if } p_n^2 < k^2 R^2 \end{cases} \quad (4)$$

where p_n is the n th root of the J_0 Bessel function.

For the case of a cavity / plasma system of infinite length (i.e., $\beta = 0$), Buchsbaum et al. [5] have undertaken a perturbation expansion of Eq. (1) assuming $p_m R/a$ to be small. This expansion is only valid for sufficiently small values of mode number m . A perturbation expansion of Eq. (1) that is valid for arbitrary values of m and R/a can be obtained by considering as the perturbation parameter $\Delta k_{0a} = k_{0a} - p_m$. For $\beta = 0$, we then obtain to first order

$$\Delta k_{0a} = \frac{\pi}{4} \left(\frac{p_m R}{a}\right)^2 \left[J_0^2\left(\frac{p_m R}{a}\right) + J_1^2\left(\frac{p_m R}{a}\right) \right] \frac{\omega_p^2}{\omega^2} \quad (5)$$

An example of the dispersion curves for the TM_{0m0} modes of a cylindrical cavity is shown in Fig. 2 for three values of R/a . Here is plotted the first seven modes for the cavity, assuming $\beta = 0$, given by the solution of Eq. (1). Also shown in Fig. 2 is the result of the perturbation theory, Eq. (5).

Two main features of the dispersion curves shown in Fig. 2 can be noted. Firstly, while for low values of m the curves are smooth, with increasing m there is a marked sharpening of the "knee" that occurs for $\omega_p^2/\omega^2 < 1$. This phenomenon is more pronounced for higher values of R/a . Indeed, for $R/a = 0.4$, there is evidence of two such "knees" for $m \geq 6$. It can be shown that the occurrence of these "knees" corresponds to $kR = p_n$, an equality that can only be satisfied, for a given value of R/a , for sufficiently high mode numbers.

Secondly, Fig. 2 shows that the range of values of ω_p^2/ω^2 for which the perturbation theory is valid depends strongly on the mode number. For example, for $R/a = 0.25$, good agreement between the solutions of Eq. (1) and Eq. (5) can be observed over a large range for $m = 1$ and $m = 6$. On the contrary, the range of validity of the perturbation theory is particularly small for $m = 1$ and $m = 7$. The range of validity is seen in general, but not always, to be greater for lower values of R/a for a given mode.

It should be noted that for $R/a = 0.25$, due to the normalization of the dispersion curves shown in Fig. 2, the range of plasma density for which the perturbation theory is valid is approximately ten times greater for $m = 6$ than for $m = 1$. In addition, it can be remarked that the critical density n_c for the $m = 6$ mode is greater than 75 times larger than for the $m = 1$ mode. Thus, for a given R/a , Fig. 2 indicates that the optimum mode for the application to the measurement of plasma density may be of higher order than $m = 1$.

The influence of the finite length of the cavity can be gauged from the curves shown in Fig. 3. Here is plotted for $m = 1$ and $m = 6$ the dispersion curves, calculated both with and without the correction term β , for a cavity with $R/a = 0.25$ and $R/d = 0.25$.

As noted by Thomassen [7], for $m = 1$ the influence of the fringing fields at the ends of the cavity is to decrease the slope of the dispersion curve for small values of ω_p^2/ω^2 . This results in a slight decrease in the sensitivity of the resonant frequency on the density of the plasma within the cavity. As observed in Fig. 3, a similar but less pronounced effect occurs for the $m = 6$ mode. In fact, for $m = 6$ the correction term β causes only a slight change in the calculated dispersion curve, even for the relatively short cavity considered in this example.

Finally, according to the analysis of Thomassen [7], Eq. (1) can be also applied to a plasma with radial non-uniformities in density provided that ω_p is calculated using the density averaged over the plasma cross-section. In the present paper it is assumed

that the plasma density is axially uniform over the length of the cavity section.

3. Experiment

3.1 Plasma production and diagnostics

The experiments were performed in a 1 m long stainless steel vacuum vessel immersed in a magnetic field generated by four large diameter water-cooled copper coils. The steady state plasma was produced by a continuous axial discharge using a radiatively-heated electron-emitting cathode. The cathode consisted of a circular nickel disc of 50 mm diameter, covered with barium, calcium and strontium carbonates which react and transform into oxides when heated to 1000 °C; a working temperature of 900 °C then being used. A maximum discharge current of 8 A and a filling gas of argon was considered for the present experiments. The resulting plasma had a radius $R = 25$ mm. A schematic diagram of the experimental arrangement is shown in Fig. 4.

A standard Langmuir probe was moved radially across the plasma to measure electron temperature and the relative density profile. The collecting area of the probe consisted of a tantalum disc of 2 mm diameter, with only the surface facing the cathode acting as the collecting electrode, the second face being covered with a ceramic layer. A sweep voltage generator constructed in-house was used to determine the conventional probe characteristics. An electron temperature in the range 2 - 5 eV, and radially-uniform in profile, was deduced from the probe characteristics. The density profile determined from the ion saturation current drawn by the Langmuir probe was found to be approximately parabolic for the entire range of discharge current considered (Fig. 5).

The average plasma density was measured by the resonant cavity technique and, for comparison, by a conventional microwave interferometer (Fig. 4). The interferometer source was a gun diode with an operating frequency of 30.5 GHz. The interferometer phase shift gave a measure of the line-integrated density across the plasma diameter.

3.2 Cavity construction

The cylindrical cavity was constructed from copper tube, with the end plates silver-soldered to provide a good electrical connection. The cavity had a radius of $a = 100$ mm, and a length of $d = 100$ mm (Fig. 1). These dimensions were chosen as a compromise of the minimization of the cavity size without excessively high values of R/a and R/d . Circular holes of 60 mm diameter were cut into the end plates to allow the free passage of the plasma column.

The TM_{060} mode of the cavity was chosen for the present experimental study for three main reasons. Firstly, the critical density for the $m = 1$ mode, for example, is $n_c = 2.0 \times 10^{10} \text{ cm}^{-3}$. This is significantly lower than the operational density range for the present device, necessitating the use of a higher order mode. For the TM_{060} mode, $n_c = 1.5 \times 10^{12} \text{ cm}^{-3}$, which is higher than the maximum density attainable in our experimental device. Secondly, the frequency range of this mode corresponding to the chosen cavity radius is 8.6 - 11 GHz (see Fig. 2). This range was covered by the high frequency sweep generator that was available in the laboratory (Weinschel model 434A, 8.0 - 12.4 GHz). Thirdly, for $R/a = 0.25$, the density range over which the perturbation theory is valid is greatest for the $m = 6$ mode, as discussed in section 2. While it is possible to solve Eq. (1) for those parameters for which the perturbation theory is not applicable, the possibility of using Eq. (5) allows the analysis of the experimental data to be greatly simplified. The TM_{060} mode therefore appears to be an optimum choice.

In order to excite the TM_{060} mode of the cavity, a small loop antenna was constructed to couple to the azimuthal magnetic field component of the mode. The antenna was placed outside the plasma column, to avoid shadowing and the drawing of current from the plasma. The antenna was positioned 47 mm from the plasma centre, that is, 22 mm from the plasma edge. This corresponds to the theoretical position of the third antinode of the cavity wavefield of the $m = 6$ mode. A second antenna was placed at an angle of 60° from the first in order to detect the cavity wavefields and therefore determine the resonant frequency.

Connections between the high frequency circuitry and the cavity positioned within the vacuum vessel were provided by vacuum type N connectors. The sweep generator was coupled to the exciting antenna through a directional coupler which allowed the continuous monitoring of the applied frequency by means of a frequency counter. The detection antenna was directly connected to a power meter. The output signals from the frequency sweep and the detection antenna were sent to a chart recorder.

Preliminary tests were performed using polystyrene foam rods of known dielectric constant. The results of these experiments showed good agreement, to within 4 %, between the measured resonant frequencies and those calculated theoretically from Eq. (1).

3.3 Results and discussion

Typical plots of the frequency dependence of the power of the cavity wavefields are shown in Fig. 6 for several values of discharge current. Sharp peaks corresponding to well-defined resonant frequencies are observed for each of the curves. This indicates that cavity modes with sufficiently high quality factors for the present diagnostic analysis can be excited over the entire range of densities considered ($n/n_c < 0.15$).

The shift in the resonant frequency measured when the plasma is introduced into the cavity can be related, using Eq. (1), to an average plasma density. For even the highest value of frequency shift measured, corresponding to the maximum discharge current of 8 A, the perturbation theory is a valid approximation. In addition, for the experimental parameters considered, the influence of fringing fields is negligible, as discussed in section 2. The same values of average density are therefore calculated independently of whether Eq. (1) or Eq. (5) is used. Calculated values of the plasma density as a function of discharge current are shown in Fig. 7. Also shown in Fig. 7 are the values of density determined using the microwave interferometer.

It should be noted that the interferometer yields line-integrated values of density, whereas the resonant cavity technique determines the density averaged over the plasma cross-section. Thus in order to compare the interferometer and cavity data, it is necessary to know the radial profile of the density. The profile is readily obtained, however, using a Langmuir probe as discussed in section 3. In Fig. 7 is shown the values of the density on the axis of the plasma column calculated by the two techniques assuming that the plasma is either uniform or has the measured parabolic profile (Fig. 5). Clearly, a better agreement is observed when the effect of the radial non-uniformity of the plasma density is taken into account.

Figure 7 shows that the density values obtained from the two diagnostic techniques, assuming the measured parabolic profile, are in good agreement over most of the range considered. For the highest values of discharge current, and hence plasma density, the agreement is poorer. The reason for this discrepancy is not clear, given that the density is much less than n_c and that the density profile remains parabolic over the entire operating range.

4. Conclusions

It has been shown in this paper that a low order TM_{0m0} mode may not always be the optimum choice for a given experimental device. Higher order modes have a higher frequency and therefore the advantage of a much greater critical density. In addition, for a judiciously chosen high order mode, the range of density for which the simple perturbation theory is applicable can be much larger.

Furthermore, it has been shown that it is possible to excite and detect high order modes - the TM_{060} mode for the present experiment. Sufficiently high cavity Q values have been obtained which allow the accurate determination of the resonant frequency, and hence of the density of the plasma contained within the cavity. Favourable comparison of density values obtained by the microwave interferometer and by the resonant cavity technique - which appears not to be available in the existing literature - has been demonstrated. This indicates that the resonant cavity can, in principle, provide a reliable diagnostic technique for the measurement of a wide range of densities in a magnetized plasma column.

Acknowledgements

This work was partially supported by the Fonds National Suisse de la Recherche Scientifique.

References

1. F. Chen, in *Plasma diagnostics*, R.H. Huddlestone and S.L. Leonard (ed.), Academic Press, New York, p. 113 (1965).
2. L. Schott, in *Plasma diagnostics*, W. Lochte-Holtgreven (ed.) North Holland, Amsterdam, p. 668 (1968).
3. S.C. Brown and D.J. Rose, *J. Appl. Phys.* **23**, 1028 (1952).
4. S.J. Buchsbaum and S.C. Brown, *Phys. Rev.* **106**, 196 (1957).
5. S.J. Buchsbaum, L. Mower and S.C. Brown, *Phys. Fluids* **3**, 806 (1960).
6. K.I. Thomassen, *J. Appl. Phys.* **34** 1622 (1963).
7. K.I. Thomassen, *J. Appl. Phys.* **36**, 3642 (1965).
8. J.H. Harris and D. Balfour, *Proc. VII Int. Conf. Phenomena in Ionized Gases*, Beograd, Vol. III, 79 (1965).
9. F.F. Chen, C. Etievant and D. Mosher, *Phys. Fluids* **11**, 811 (1968).
10. B.I. Ivanov, *Sov. Phys. - Tech. Phys.* **15**, 377 (1970).

Figure Captions

- Fig. 1. Schematic diagram of the HF resonant cavity.
- Fig. 2. Dispersion curves for the first seven TM_{0m0} modes, calculated for (a) $R/a = 0.1$; (b) $R/a = 0.25$; and (c) $R/a = 0.4$. The solid curves were calculated from Eq. (1), while the broken lines were obtained from perturbation theory, Eq. (5).
- Fig. 3. Dispersion curves for (a) TM_{060} and (b) TM_{010} , calculated assuming a cavity of infinite length (solid curves) and a finite length cavity with $R/d = 0.25$ (broken curves).
- Fig. 4. Schematic layout of the experimental apparatus.
- Fig. 5. Measured radial profile of the plasma density for three values of discharge current (\bullet $I_p = 1$ A; ∇ $I_p = 3$ A; and $+$ $I_p = 5$ A).
- Fig. 6. Frequency dependence of the power of the cavity wavefields measured for several values of discharge current, I_p .
- Fig. 7. Comparison of the density on the axis of the plasma column measured by the resonant cavity technique (squares) and by microwave interferometry (circles). The open symbols represent values obtained assuming a uniform density profile, whereas the solid symbols were obtained assuming the measured parabolic profile.

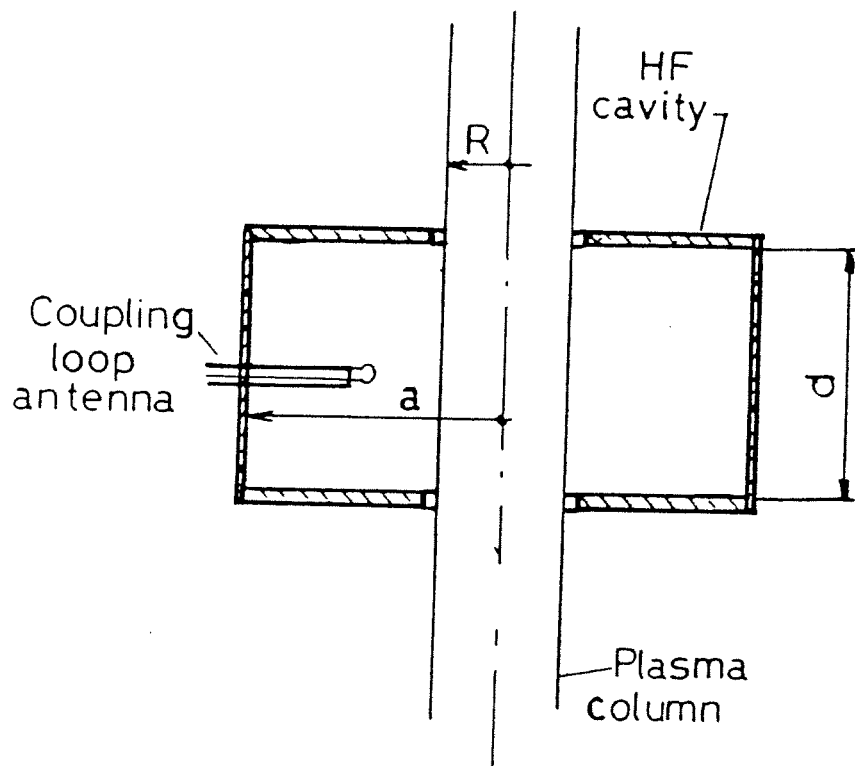


Fig. 1

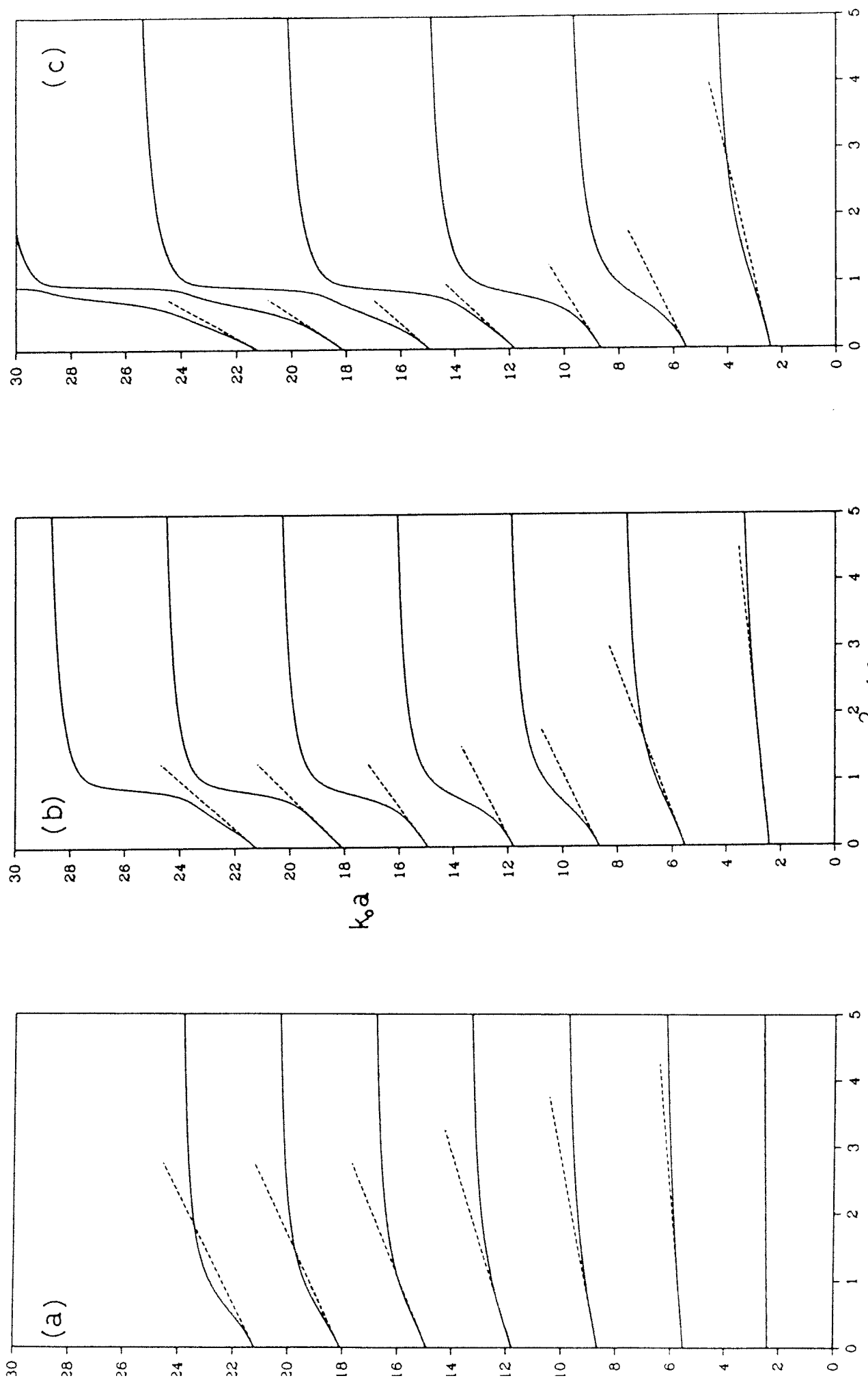


Fig.2

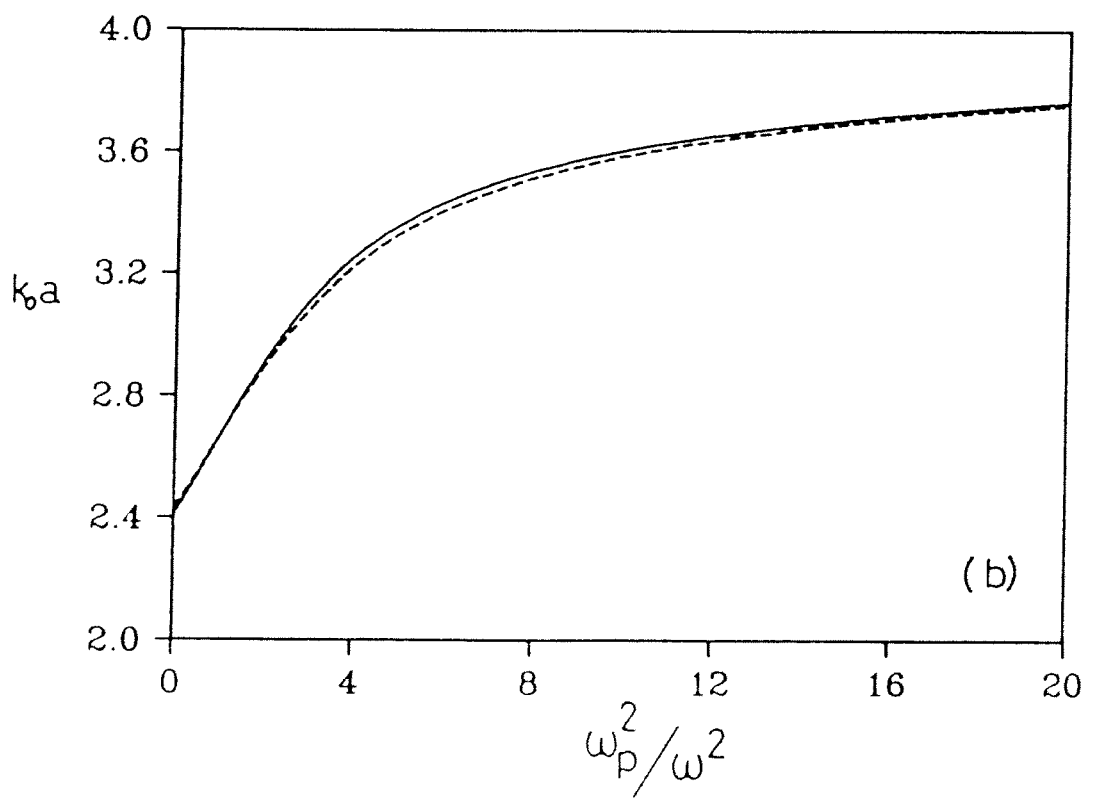
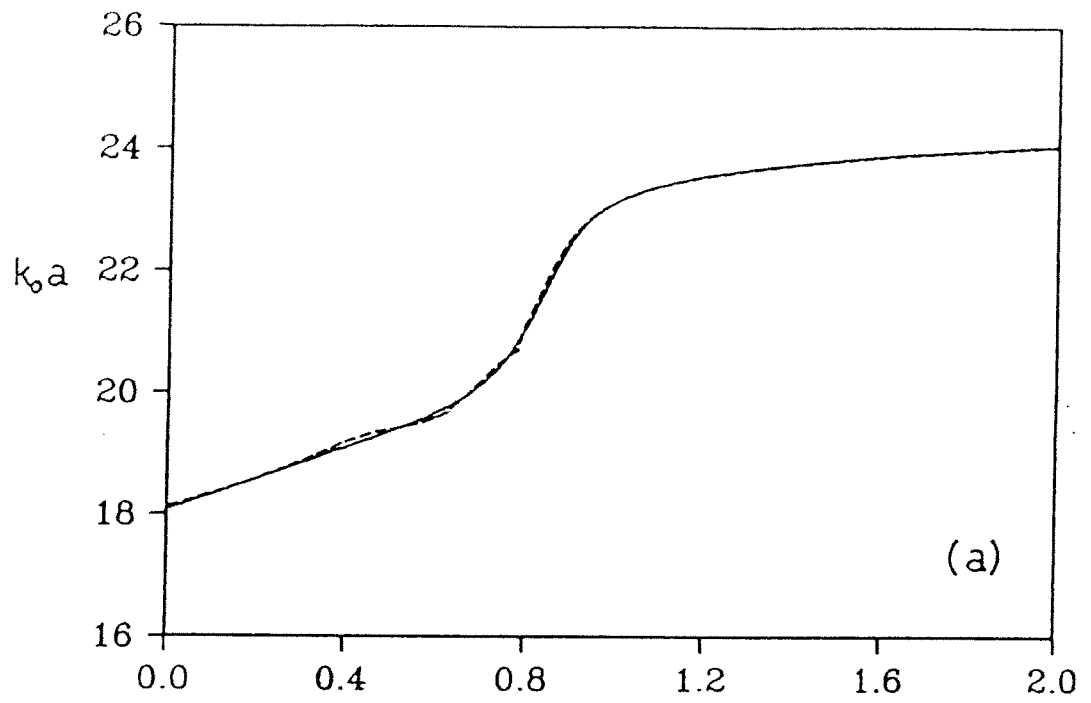


Fig. 3

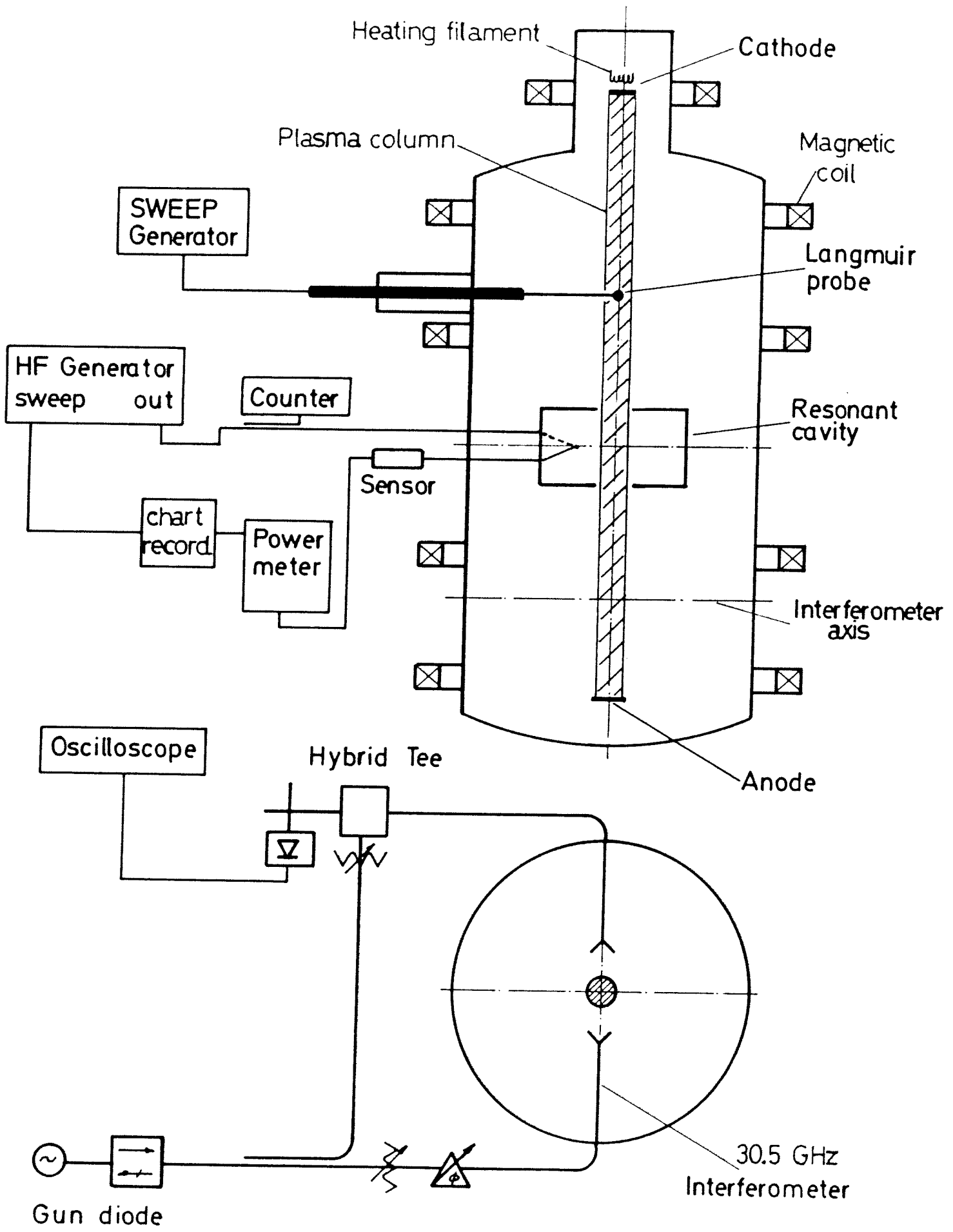


Fig. 4

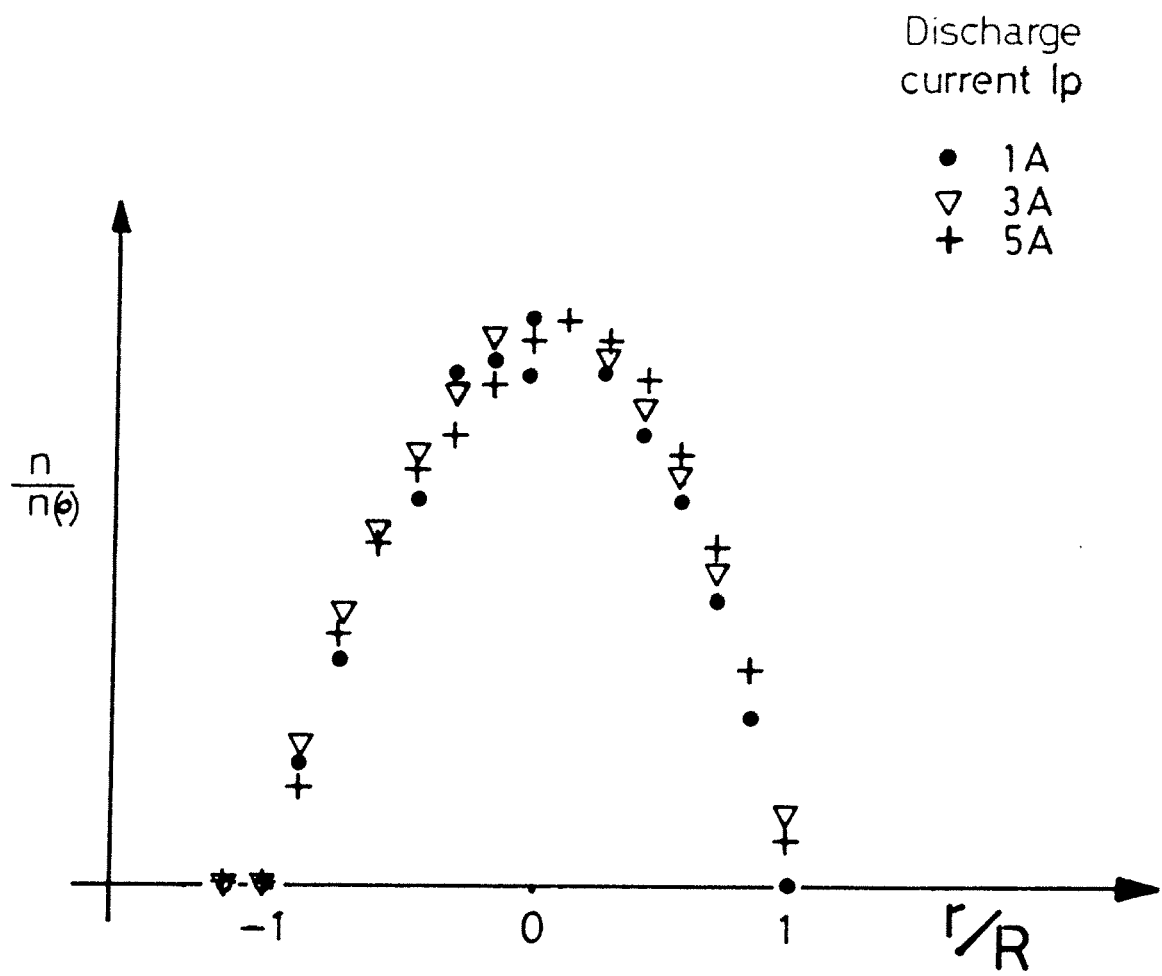


Fig. 5

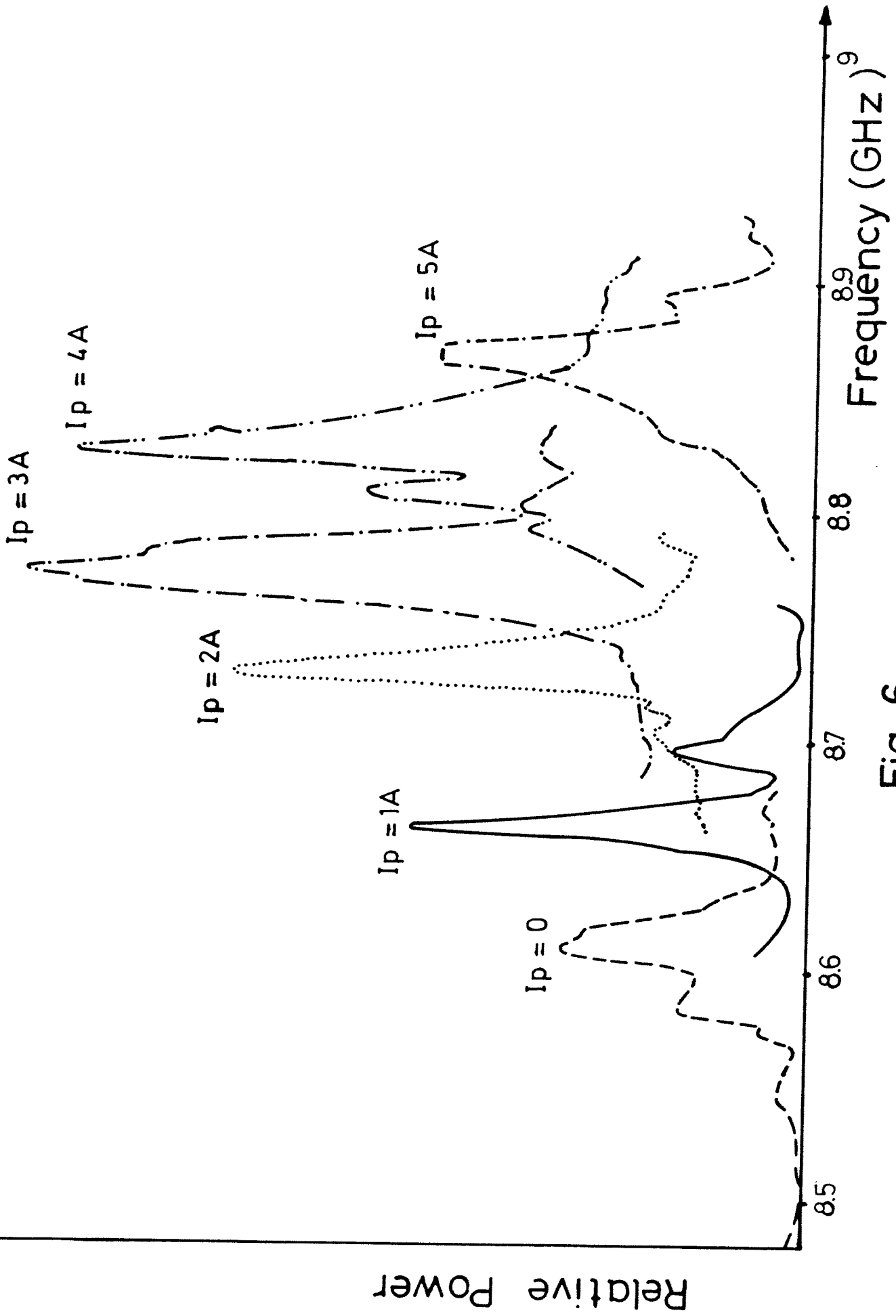


Fig. 6

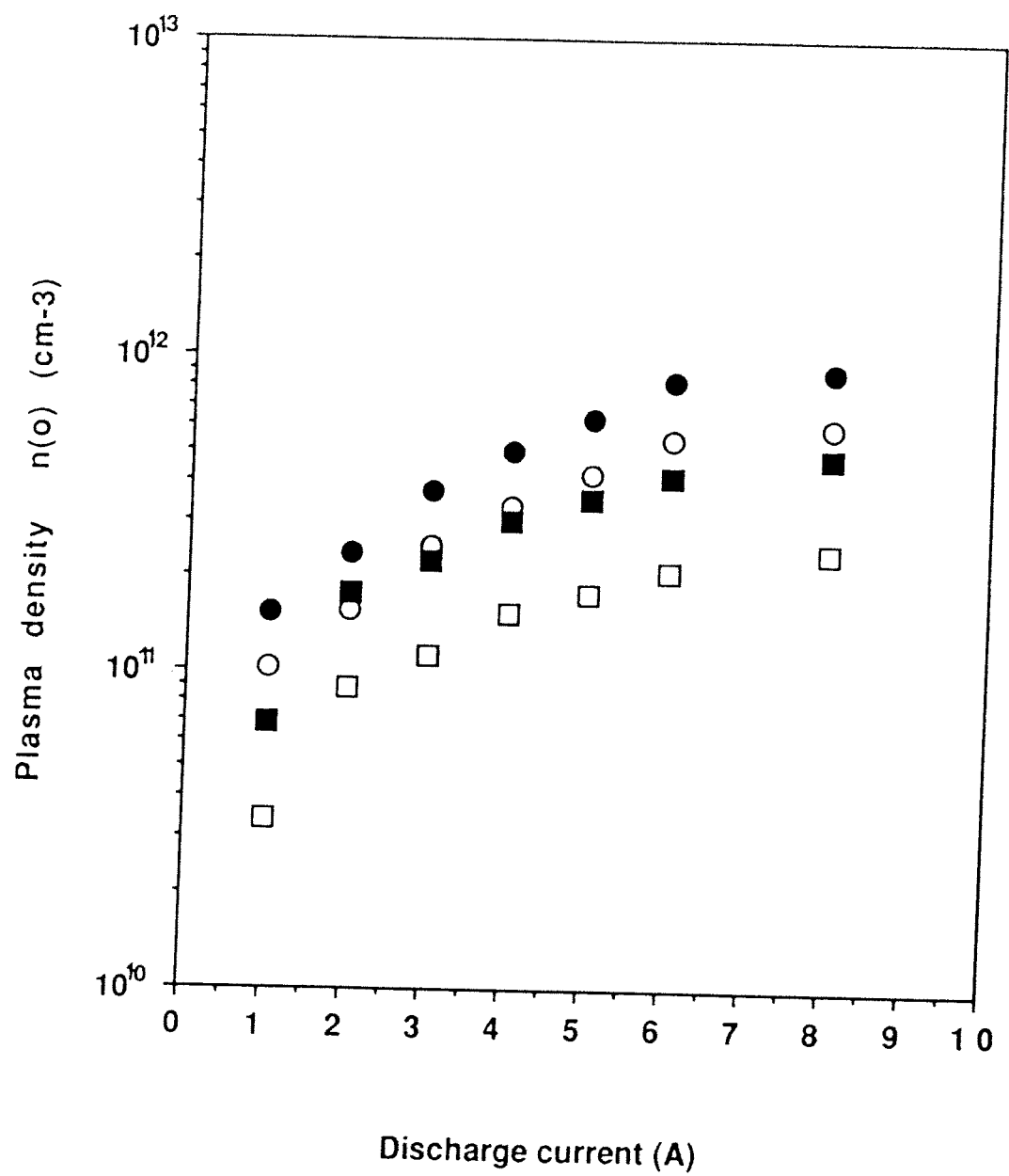


Fig. 7

